

# Calculation of Collision Speed Corresponded to Maximum Penetration Using Hydrodynamic Theory

A.R. Nezamabadi \*

*Department of Mechanical Engineering, Islamic Azad University, Arak Branch, Arak, Iran*

Received 10 August 2016; accepted 15 October 2016

## ABSTRACT

One of the most valid and efficient models of long rod projectile penetration in homogeneous targets is Tate and Alekseevskii's (A&t) model. Based on Tate's model, the present research tries to calculate the optimum speeds to achieve the maximum penetration depth in the homogeneous targets. The proposed collision speed-penetration depth diagrams are developed using Tate's model. In this way, various collision speed-penetration depth diagrams for different projectile dynamic resistances and targets are calculated and the optimum speed envelope is derived. According to Tate's diagrams, the increase of collision speed is not followed by the increase of penetration depth; instead, it causes erosion phenomenon to happen. The comparison of the resulted optimum penetration speeds and the available data confirms the findings. Speed and rigidity both have a positive impact on the increase of penetration depth. With the increase of speed, the erosion issue finds a higher significance due to the increase of pressure on the projectile tip. Therefore, higher speed and erosion are opposed to each other; for the case of  $Y > R$ , there are some maximum points which indicate the optimum reciprocity of the two mentioned factors to obtain a maximum penetration depth. In the present research, an equation is developed indicating the optimum speeds resulting in the maximum penetration rate in the case of  $Y > R$ . For the reciprocity of speed and erosion, the target resistance against an erosive projectile should be 4 to 5 fold higher than the same target resistance against a rigid projectile penetration. [1] © 2016 IAU, Arak Branch. All rights reserved.

**Keywords :** Hydrodynamic theory; Tate and Alekseevskii's theory; Erosion; Rigidity; Optimum speed; Maximum penetration depth.

## 1 INTRODUCTION

**W**HEN a projectile penetrates into a semi-infinite concrete target, it continuously pushes the target materials and drives it toward a radius of its front section [2-5]. If the pressure applied on the contact point between the projectile tip and the target is higher than the projectile resistance, its tip deformation will happen and it changes to a mushroom-like shape (mushrooming phenomenon). This deformation varies depending on collision speed as well as projectile and target relative resistances. For collision speeds lower than 1000m/s, there is no significant deformation in the projectile [2], so in this case the hypothesized undeformability of projectile tip will be met. In such a case, there is a linear relation between the penetration depth and collision speed [2] which is calculated using the expansion theory for concrete target resistance cavity against the movement of rigid projectile and ultimately, the penetration depth is calculated.

\*Corresponding author. Tel.: +98 86 34130022; Fax: +98 8634130023.  
E-mail address: a-nezamabadi@iau-arak.ac.ir (A.R.Nezamabadi).

## 2 RELATION BETWEEN COLLISION SPEED AND EROSION PHENOMENON

With the increase of collision speed, the erosion phenomenon begins at the projectile, its tip changes to mushroom form and its materials are ejected into the surrounding environment. It causes some wasting in energy along with an outstanding efficiency reduction of projectile penetration into the target. Unfortunately, there is a lack of experimental data about the penetration into the concrete targets at 1000m/s or more speeds. The extant data for tungsten and tantalum projectiles relates to 3900m/s to 4600m/s collision speeds [5]. The penetration depth into concrete target is proportional to reduction in the length of projectile rode indicating an agreement with the penetration hydrodynamic theory. Using reverse ballistic experiments, Miler and Mckay tried to study the penetration of tungsten projectiles at 900 m/s to 4300m/s speeds. Although there is a dispersed data in this respect, it shows an acceptable agreement with hydrodynamic theory. The present relatively scant data for collision speeds lower than 2000m/s indicates the reduction of cavity diameter in the target (decrease of mushrooming phenomenon). The fact reveals the possibility of intermediate cases and expression of the projectile and target resistances impacts. What is studied and tested in the present research relates to collision speeds higher than 1200m/s to 1600m/s. In such speeds, the projectile and target resistances are manifested and so should be considered in the equations. It is thus inevitable to use the penetration equations developed by Tate and Alekseevskii instead of hydrodynamic theory.

## 3 EROSIIVE PENETRATION MODEL AND HYDRODYNAMIC THEORY

The above mentioned facts lead us to use the erosive penetration model for long rod projectiles in the semi-infinite concrete target considering resistance impacts of projectile and target.

The solution of the following equation is used to obtain a closed solution for  $l$  [6-9].

$$Y + \frac{1}{2} \rho_p (v-u)^2 = \frac{1}{2} \rho_T u^2 + R \quad (1)$$

$$Y = -\rho_p l \frac{dv}{dt} \quad (2)$$

$$\frac{dl}{dt} = -(v-u) \quad (3)$$

$$\frac{dl}{l} = \frac{\rho_p (v-u)}{Y} dv \quad (4)$$

The following equation can be solved,  $l$  to obtain closed form.

$$\frac{dl}{l} = \frac{\rho_p \left( v - \frac{v - \mu(v^2 + A)^{\frac{1}{2}}}{1 - \mu^2} \right)}{Y} dv \quad (5)$$

The equations  $A, \mu, u$  are defined as follows:

$$u = \frac{v - \mu(v^2 + A)^{\frac{1}{2}}}{1 - \mu^2}, \quad \mu = \left( \frac{\rho_T}{\rho_p} \right)^{\frac{1}{2}}, \quad A = \frac{2(R - Y)(1 - \mu^2)}{\rho_T} \quad (6)$$

Based on the relation,  $l$  is derived according to  $v$  and  $v_0$ . For  $R < Y$ , the penetration depth is obtained from the following integral.

$$P = \frac{\rho_p}{Y_p} \int_{v_0}^{v_{cr}} u l dv = \frac{\rho_p}{Y_p} \int_{v_0}^{v_{cr}} \frac{v - \mu(v^2 + A)^{\frac{1}{2}}}{1 - \mu^2} l(v, v_0) dv \tag{7}$$

Since, so the above relation is considered as a function of following variables:

$$\frac{P}{L} = F(v_0, \rho_p, \rho_t, R, Y_p) \tag{8}$$

It means that for constant  $\rho_t, \rho_p$  and  $R$ , it is possible to obtain corresponding values for each  $Y$  in lieu of variable  $v_0$ . For instance, for  $\rho_p = \rho_t = 7850$  and  $R = 50MPa$  with  $v_0 > v_{cr}$ , the following Fig.1 is obtained (in which  $Y =$  variable,  $R = cte$ , vertical axis shows  $P/L$  ratio and horizontal axis indicates  $v_0$  value).

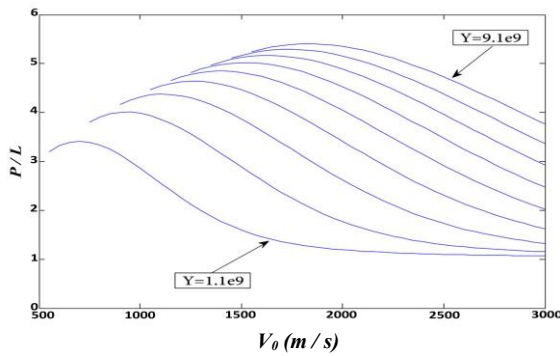


**Fig.1**  
Aspect ratio  $P/L$  in terms of the initial velocity of the projectile, in the case of  $Y$  variable and constant  $R$ .

As it can be seen from the Fig.1,  $Y = 1.1e9$  changes to  $Y = 9.1e9$ . Toward the right side of the figure, diagrams show the increase of  $Y$ .

It is possible to draw the diagram with a changing  $R$  and a constant  $Y$ . For example, for a constant  $\rho_p = \rho_t = 7850$  and  $Y = 500MPa$  with changing  $R$ , the following Fig.2 is obtained for each changing  $v_0$ 's (in which  $Y =$  variable,  $R = cte$ , vertical axis shows  $(P/L)$  ratio and horizontal axis indicates  $v_0$  values).

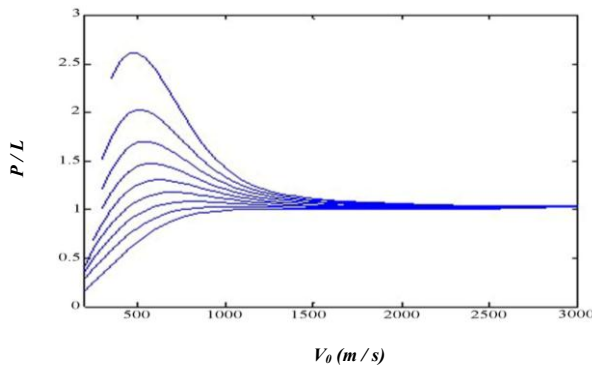


**Fig.2**  
Aspect Ratio  $P/L$  in terms of the initial velocity of the projectile, in the case of  $R$  variable and constant  $Y$ .

As it can be seen in the Fig.2,  $R = 0.5e8$  changes to  $R = 4.5e8$ . In the bottom of the figure, diagrams show the increase of  $R$ . Here, the main purpose is to drive a relation for each specific  $\rho_p, \rho_t$  and to calculate  $v_0$  value according to the maximum penetration depth which for simplicity is called  $v_m$  and also to determine its corresponding maximum penetration value,  $P_m$ . The above figures show that effectiveness of changing in  $Y$  on  $v_m$  is more than  $R$ .

The important point here is that with regard to the extant relations, the maximum is achieved only with  $R < Y$ . Using Lybernitz relation, differentiation of penetration depth integral gives:

$$P = \int_{v_0}^{v_{cr}} G(v, v_0) dv \Rightarrow \frac{\partial P}{\partial v_0} = \int_{v_0}^{v_{cr}} \frac{\partial G}{\partial v_0} dv - L = 0 \tag{9}$$

In this way, the above equation is solved as an integral equation. Based on the complex formulation of function  $G$ , it is not possible to calculate the integral as usual (except under specific conditions). Therefore, the integral is drawn using numerical method for different  $R$  and  $Y$  values. In the following Fig.3, the maximum values of  $R$  and  $Y$  are connected through straight lines.

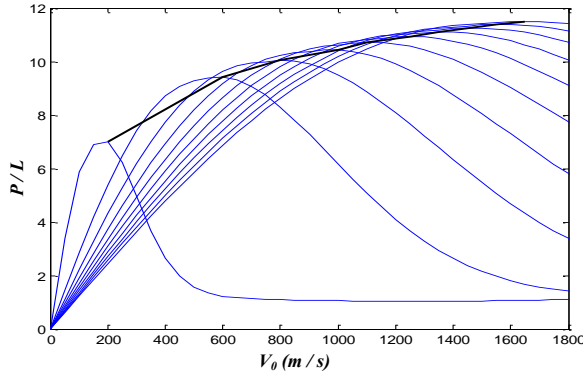


**Fig.3** Aspect Ratio  $P/L$  in terms of the initial velocity of the projectile.

As it can be observed, the maximum values are not positioned in a straight line. The Fig.3 is drawn for different  $R$  and  $Y$  values and similar to the above procedure, the maximum values are connected through straight lines. For more simplicity, only maximum values are marked. It is worth mentioning that  $\rho_p = \rho_t = 7850$  are selected for the following Fig.4.

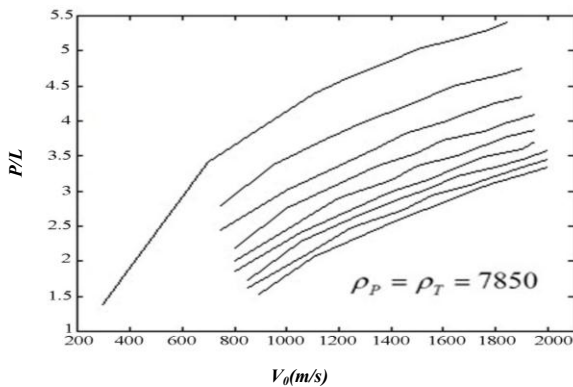


**Fig.4** Aspect Ratio  $P/L$  in terms of the initial velocity of the projectile, in the case of  $\rho_p = \rho_t = 7850$ .

Regarding the marked points, different curves were tested for fitting purposes and finally a curve with the below pattern was selected as the curve with highest goodness of fit and lowest error. It is necessary to mention that individual relations are proposed:

$$x_1 = \ln(R_t) \quad ; \quad x_2 = \ln(Y_p)$$

$$\ln(v_m) = a_0 + a_1 x_1 + a_2 x_2 + a_3 x_1^2 + a_4 x_2^2 + a_5 x_1 x_2$$

$$(P/L)_m = a_0 + a_1 x_1 + a_2 x_2 + a_3 x_1^2 + a_4 x_2^2 + a_5 x_1 x_2$$

Coefficients for each term are given in the following Table.1:

**Table1**

Coefficients  $a_0$  to  $a_5$  in the presented model to get the second  $v_m, (P/L)_m$ .

	$a_0$	$a_1$	$a_2$	$a_3$	$a_4$	$a_5$
$v_m$	0.7506	0.1146	0.0020	0.0048	0.0142	-0.0106
$(P/L)_m$	1.2779	-0.8038	0.7723	0.0076	0.0105	-0.0179

In the following Fig.5, the resulted curve obtained from the above fitted curve is shown comparing  $v_m$  primary data. The error rate resulted from the above examination of fit goodness is 0.8764 percent (vertical axis in Fig.5,  $v_m$  ration and horizontal axis indicates  $(P/L)_m$  values).

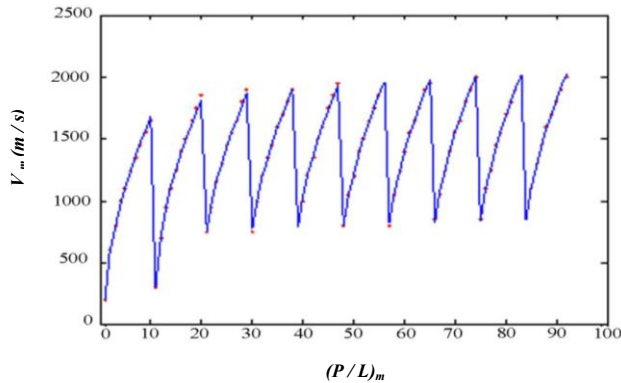


**Fig.5**  
The curve fitting, considering the data  $v_m, (P/L)_m$ .

The following Fig.6 also reveals the resulted curve obtained from the above fitted curve for  $(P/L)_m$  primary data (vertical axis in Fig.6,  $v_m$  ration and horizontal axis indicates  $(P/L)_m$  values).

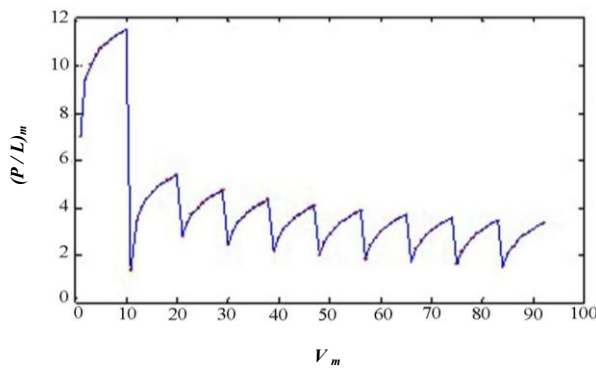


**Fig.6**  
The following figure also reveals the resulted curve obtained from the above fitted curve for  $(P/L)_m$  primary data.

For example, assume  $R = 200MPa$  and  $Y = 500Mpa$ . Thus:

$$x_1 = Ln(R_p) = 19.1138 \quad ; \quad x_2 = Ln(Y_p) = 20.0301$$

Using the first row in the above mentioned table:

$$Ln(v_m) = a_0 + a_1x_1 + a_2x_2 + a_3x_1^2 + a_4x_2^2 + a_5x_1x_2 = 6.3774 \Rightarrow v_m = 588.3676$$

and according to the second row in the table, we have:

$$(P/L)_m = a_0 + a_1x_1 + a_2x_2 + a_3x_1^2 + a_4x_2^2 + a_5x_1x_2 = 1.5231$$

Figs.7 and 8, which are the main references, confirms the results obtained in the simulation model.

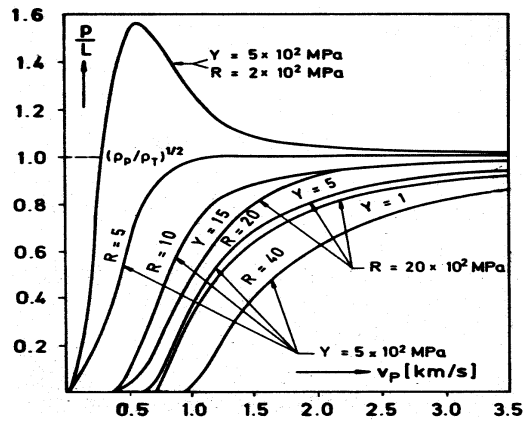


Fig.7  
Penetration curves calculated for  $\rho_p = \rho_T, R \geq Y$  [10,11].

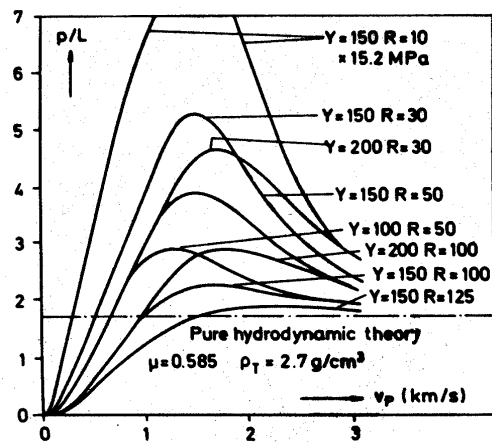


Fig.8  
Penetration curves calculated for  $R < Y$  [10,11].

#### 4 CONCLUSIONS

When there are extreme points in the Tate graphs and  $R$  is greater than that of  $Y$ , the projectile is rigid enough. Therefore, proportional to the projectile rigidity, optimized velocity has a lot to shoot with the speed and will cause optimal performance of the projectile and will get the maximal depth. In This paper, curve fit equation obtained from this particular case is not bound trapped. Thus, it can be used for designing the resistance of the target projectile in this paper. In addition to gained results, it is acceptable to emphasize the capability of Tate graphs because we managed to do a kind of optimization and estimate the maximal depth and obtain optimized speed as well.

#### REFERENCES

- [1] Rosenberg and Z., Dekel E., 2008, A numerical study of the cavity expansion process and its application to long-rod penetration mechanics, *International Journal of Impact Engineering* **35**: 147-154.
- [2] Forrestal M. J., Frew D. J., Hickerson J. P. Rohwer T. A., 2003, Penetration of concrete targets with deceleration-time, *International Journal of Impact Engineering* **28**: 479-497.
- [3] Frew D.J., Forrestal M.J. Cargile J.D., 2006, The effect of concrete target diameter on projectile deceleration and penetration depth, *International Journal of Impact Engineering* **32**: 1584-1594.
- [4] Forrestal M. J., Frew D. J., Hanchak S. J. Brar N. S., 1996, Penetration of grout and concrete targets with ogive-nose steel projectiles, *International Journal of Impact Engineering* **18**: 465-476.

- [5] Vladimir M.G., 1996, Concrete penetration by eroding projectiles: experiments and analysis, Technical Report ARAED-TR-96014.
- [6] Alekseeveskii V.P., 1966, Penetration of a Rod into a Target at High Velocity, *Combus Explos Shock Waves* **2**: 63-66.
- [7] Dullum O., Haugstad B., 1981, *On the Effect of Finite Strength in Long Rod Penetration*, Forsvarets Forskningstitutt, FFI/Rapport-81/4001, Kjeller, Norway .
- [8] Tate A., 1967, A theory for the deceleration of long rods after impact, *Journal of the Mechanics and Physics of Solids* **15**: 387-399.
- [9] Tate A., 1969, Further results in the theory of long rod penetration, *Journal of the Mechanics and Physics of Solids* **17**: 141-150.
- [10] Zukas J. A., 1990, *High Velocity Impact Dynamics*, John Wiley & Sons.
- [11] Williams A. E., 1976, Impact tests with mathematics method , *Proceedings, 27th Meeting of the Aeroballistic Range Association*, Centre, d Etudes de Vaujourns, Sevran, France.